J. Fluid Mech. (2017), *vol.* 830, *pp.* 326–349. © Cambridge University Press 2017
doi:10.1017/jfm.2017.488

Surface shape stability analysis of a magnetic fluid in the field of an electromagnet

T. I. Becker[1,†], V. A. Naletova[2,3], V. A. Turkov[3] and K. Zimmermann[1]

[1]Technical Mechanics Group, Faculty of Mechanical Engineering, Technische Universität Ilmenau, Max-Planck-Ring 12, 98693 Ilmenau, Germany

[2]Department of Hydromechanics, Faculty of Mechanics and Mathematics, Lomonosov Moscow State University, Leninskiye Gory, 119991 Moscow, Russia

[3]Insitute of Mechanics, Lomonosov Moscow State University, Michurinskiy pr. 1, 119192 Moscow, Russia

(Received 27 December 2016; revised 29 May 2017; accepted 12 July 2017; first published online 29 September 2017)

Static surface shapes of a magnetic fluid volume between two plates in a non-uniform magnetic field are investigated theoretically and experimentally. Abrupt changes and hysteresis of the magnetic fluid surface shape are observed in the experiments when the current in the coil increases and decreases quasi-statically. The necessary and sufficient conditions for a local minimum of the energy functional are derived theoretically. A method to find stable/unstable surface shapes is developed. The ambiguity in the determination of the magnetic fluid surface shape at the same value of the current is shown. It is found that the experimentally observed surface shapes of the given magnetic fluid volume coincide with the shapes obtained numerically, and practically all of them satisfy the derived necessary and sufficient conditions of the minimum energy. The stability curves of the magnetic fluid bridge between the plates are determined experimentally and theoretically.

Key words: liquid bridges, magnetic fluids, variational methods

1. Introduction

The free surface of a magnetic fluid (MF) subjected to a magnetic field may have interesting forms, peaking patterns and labyrinth structures (Rosensweig 1985; Abou, Wesfreid & Roux 2000; Zahn 2001). In certain situations, rapid abrupt behaviour and also hysteresis of the MF surface take place, even if the applied magnetic field is changed slowly, in a quasi-static manner. This can be explained by the ferrohydrodynamic instability of the volume shape caused by the magnetic field. In general, hysteresis is a common phenomenon in physics, fluid mechanics, biology and so on, which indicates dependence of the state of a nonlinear system on its history. In this paper, two different types of hysteresis will be considered. First, the hysteresis of an MF equilibrium surface shape between two solid plates due to the co-existence of several stable solutions for fixed parameters of the system is investigated. And second,

† Email address for correspondence: tatiana.becker@tu-ilmenau.de

the contact angle hysteresis – that is, the difference of the advancing and receding contact angles at the three-phase contact line, is considered. This effect is normally attributed to surface roughness and influence of solutes in the fluid (e.g. surfactant of the MF), which may deposit a thin film on the solid surface (de Gennes 1985).

To begin with, let us give some examples. The surface shape of an MF drop with large magnetic permeability immersed in another liquid of the same density changes its form abruptly for a certain threshold value of an increasing uniform magnetic field (Bacri & Salin 1982; Afkhami *et al.* 2010). The drop jumps spontaneously from a slightly elongated shape to a much more elongated shape due to the presence of the competing capillary and magnetic stresses at the interface. When decreasing the magnetic field, the inverse feature (shortening) occurs, but for a smaller threshold value. This is related to the fact that in a certain field range two stable shapes of the drop exist, and it depends on the initial conditions as to which solution is observed. A similar hysteresis phenomenon of a semi-infinite MF layer on a horizontal plate in a perpendicular uniform magnetic field is studied by Cowley & Rosensweig (1967), Gailitis (1977), Richter & Lange (2009). In this classical problem, known as the Rosensweig instability, the pattern-forming peaks occur on the free surface when a critical value of the vertical magnetic field is exceeded.

In essence, an MF equilibrium shape under a magnetic field is accomplished by the balance between capillary, hydrostatic and magnetic stresses. To get a qualitative notion of the problem, consider a finite MF drop on a horizontal plate under the influence of gravity and a vertical uniform magnetic field. The increase of the field strength leads to the change of the drop surface that requires, obviously, energy costs to lift up the fluid against gravity and to extend the surface area. Therefore, both gravity and surface tension have a stabilising influence on the drop shape. However, the deformed MF surface causes non-uniform distortion of the applied uniform magnetic field inside the MF. The field-induced destabilisation results in a loss of the magnetic energy due to the increased magnetisation of the fluid, and this energy change is interrelated with the drop shape. So, the MF equilibrium surface is formed, if the loss of energy because of the destabilising magnetic field balances the gain of energy due to gravity and surface tension. This explains the appearance of a conical peak with the sharp increase of the curvature at the upper point of the drop (Arkhipenko, Barkov & Bashtovoi 1980). Note that when imbalance of these energies occurs, the uniform magnetic field can lead to instability of the MF. It is shown experimentally by Barkov & Berkovskii (1980) that when the field magnitude surpasses a certain critical value, the drop splits spontaneously into two parts of approximately equal volume in a direction perpendicular to the field.

The use of non-uniform magnetic fields of different configurations extends the class of problems in which abrupt behaviour and hysteresis phenomena are observed. For example, a number of publications are devoted to the problem of an MF volume near a vertical line conductor for different particular cases (Rosensweig 1985; Bacri *et al.* 1988; John, Rannacher & Engel 2007; Naletova *et al.* 2008; Vinogradova *et al.* 2013). The stepwise change of the thickness of a hydro-weightless MF drop surrounding the conductor in response to a quasi-static increase in current is observed experimentally by Bacri *et al.* (1988) for small magnetic fields, when the magnetic permeability of the MF is constant. The theoretical analysis of this phenomenon is given by Naletova *et al.* (2008), Vinogradova *et al.* (2013) for arbitrary magnetic fields, when the MF magnetisation depends nonlinearly on the field strength. The free surface of an MF that contains a cylindrical body made of a well magnetisable material in a uniform magnetic field is investigated by Naletova *et al.* (2012). It is shown that at the same

applied value within a certain field range, solutions of different type are realised. The abrupt behaviour and hysteresis of the MF surface are experimentally revealed in the presence of a cyclically changed magnetic field.

The equilibrium surface shape of a heavy MF in the non-uniform field of a horizontal line conductor is studied theoretically in the non-inductive approximation by Kiryushin & Bin (1980), Volkova & Naletova (2014). Spasmodic and hysteretic changes of the MF shape with gradual change of the current are predicted. Volkova & Naletova (2014) solved the problem considering a finite MF volume between two limiting horizontal plates placed under the conductor accounting for surface tension. It is shown that at a fixed current, several simply connected solutions of the MF surface shape exist that are energetically favourable. In particular, there exists a so-called magnetic fluid bridge (MFB) between the horizontal plates.

Generally, a fluid bridge (or liquid meniscus) is a specifically shaped volume of fluid in contact with two solid surfaces in a short distance. It is formed during the process of coalescence of two separate fluid volumes or from a single volume due to capillary, inertia, gravity and other effects. In the moment of formation, before the bridge comes to rest as well as right after its break-up, certain small oscillations of fluid surface can be observed. The bridge is held mainly by intermolecular stresses at the fluid–air (or fluid–fluid) interface and surface tension stresses at the three-phase contact line. Static and dynamic properties of fluid bridges and, more particularly, their surface shape have been studied since the nineteenth century (Plateau 1863; Yildirim & Basaran 2001). At present, there are many applications involving fluid bridges, e.g. printing, coating, heat transfer and conductivity measurements.

In applications based on MF such as liquid acoustic ducts, seals and valves, the volume of the MFB provides a complete hermetic contact in the slot gap between the moving surfaces of a device. The MFB is held and controlled by external sources of a magnetic field, such as permanent or electromagnets. As was mentioned above, the surface shape of the MFB may change gradually under an applied alternating magnetic field. When the magnetic field reaches some critical threshold, the volume may become unstable and disintegrate, thus disrupting the operability of a device. Therefore, these effects must be considered in designing and controlling systems based on MF.

Rothert & Richter (1999) carried out experiments on the break-up of an MFB between non-magnetic horizontal plates in magnetic fields of two electromagnets and a pair of Helmholtz coils. The evolution of the minimum neck diameter and the dynamics of the satellite drop after the decay of the MFB are observed. Polevikov & Tobiska (2005) studied numerically the behaviour of an MFB in a small gap between two parallel plates subjected to a uniform magnetic field. It is shown that two different types of instabilities arise as the intensity of the magnetic field increases. For small contact angles, the MFB breaks along the capillary axis and spreads over the capillary walls, whereas for large contact angles the MFB elongates in the central part up to its separation from the walls.

From the point of view of technical applications, however, not the instability, but the stability of an MF is of great importance. Therefore, in this work, we present methods, which make it possible to determine the regions of stability of an MF equilibrium surface, in particular of the MFB, which paves the way to the use of such fluids in applications. The theoretical analysis will be based on the energy formulation of the problem using variational methods. In the works by Bacri & Salin (1982), Bacri *et al.* (1988), Rosensweig *et al.* (2005), John *et al.* (2007), equations of a static MF surface shape are also derived from the balance between gravitational, surface and

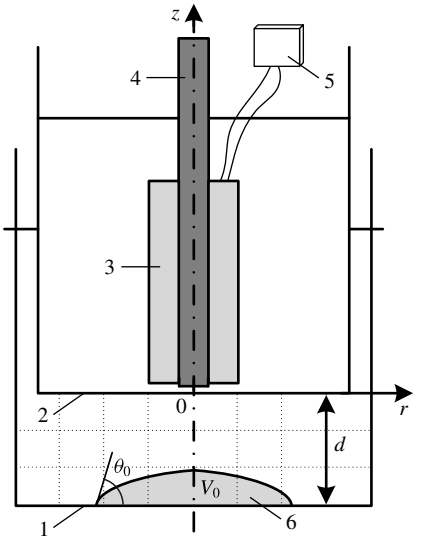

FIGURE 1. Schematic view of the experimental set-up: 1 – horizontal plate of the outer vessel, 2 – horizontal plate of the inner vessel, 3 – electromagnetic coil, 4 – ferrite core, 5 – current source, 6 – MF volume V_0.

magnetic energy terms with the condition that the total energy is stationary on the solutions. But such formulation of the problem is incomplete, since the total energy in the equilibrium state must be minimum. That means the sufficient conditions of the energy minimum should be considered. An attempt to derive and apply these conditions has been made in a previous paper by Volkova & Naletova (2014) for the two-dimensional problem of the MF surface shape in the field of a horizontal line conductor.

In the present paper, the static surface of a finite axisymmetric MF volume between two horizontal plates is investigated theoretically and experimentally in a magnetic field of an electromagnetic coil placed above the upper plate. This study continues and expands the research initiated by Volkova, Naletova & Turkov (2013), where preliminary investigations into the experimental techniques were made. Section 2 describes an experimental study which aims to obtain equilibrium surface shapes of the MF volume and to observe their abrupt and hysteretic behaviour. The variational formulation of the problem along with the necessary and sufficient conditions for the minimum energy are presented in § 3. The stability of the static, simply connected MF shapes relative to axisymmetric surface perturbations is investigated. Results of the numerical calculations and their comparison with the experimental data are discussed in § 4. In our opinion, the proposed stability analysis of MF surface shape can serve as a tool for understanding the behaviour of these fluids.

2. Experimental investigations of an MF equilibrium shape

2.1. *Experimental set-up and materials*

The experimental set-up shown in figure 1 consists of an acrylic glass inner and outer cuboidal vessels with the following dimensions: $(L \times W \times H)$ $7.3 \times 7.3 \times 9$ cm^3 and $8 \times 8 \times 8$ cm^3, respectively (Volkova *et al.* 2013). The thickness of the glass is 2.5 mm. The inner vessel is inserted vertically into the other up to the required

Carrier liquid	Water
Particle material	Magnetite
Density, ρ_1	1.1 g cm^{-3}
Saturation magnetisation, M_{1S}	12 G
Magnetic susceptibility, χ	0.03
Volume concentration, φ	0.02

TABLE 1. MF properties.

distance d between their horizontal plates. The distance d can be changed from 0 to 6 cm in steps of 1 mm. The cylindrical coordinates (r, ϕ, z) are introduced with the origin in the middle of the upper plate. The z axis coincides with the axis of symmetry of the coil, see figure 1.

The electromagnetic coil with the inserted ferrite core with soft magnetic properties of low coercivity is fixed in the inner vessel, so that the axis of symmetry of the coil is perpendicular to the upper horizontal plate through its centre. Parameters of the coil are: height 4.6 cm, inner and outer radii 0.4 cm and 1 cm, respectively. The winding of the coil is made of 270 turns of a copper wire with a diameter of 1.04 mm. The ferrite core has a radius of 0.4 cm and a height of 12.5 cm, the relative permeability of the material is 400. Its lower end extends out of the coil for 1 mm. The current source provides a range of output currents in the coil $i = 0$–2.6 A. The distribution of the magnetic field in the area between two horizontal plates is measured with an analogue Hall sensor in the absence of the MF. The maximum magnitude of the magnetic field strength $\boldsymbol{H}$ is up to 655 Oe for $i = 2.6$ A measured directly under the upper plate.

An MF volume V_0 is injected in the middle of the working area, which is the area between the horizontal plates $z = 0$ and $z = -d$ of the experimental set-up. In order to reduce capillary and gravitational forces, the area was first filled with a non-magnetic liquid (NML) with a density smaller than the MF.

Experimental results were carried out using a water-based MF and polymethylsilicone liquid as an NML. This combination is chosen due to the fact that these fluids are immiscible, and the MF does not stain the walls of the vessel. The parameters of the MF are listed in table 1. This low concentration fluid has a small value of the saturation magnetisation and, therefore, the normal-field instability of the surface in applied magnetic fields was not observed. The polymethylsilicone liquid has the following parameters: the density is $\rho_2 = 0.91$ g cm^{-3}, the kinematic viscosity 5.5 cSt. The surface tension coefficient on the interface between these fluids is measured by the pendant drop method: $\sigma = 11.7$ g s^{-2}.

2.2. *MF volume in a step-like increasing and decreasing magnetic field*

The experimental results of the MF behaviour between the horizontal plates when the current in the coil increases and decreases quasi-statically are presented. In each experimental series, the distance between the plates is fixed to $d = 1.2$ cm. An MF volume V_0 is initially injected in the middle of the lower plate when the current in the coil is turned off. Then the current is increased in steps of 0.001–0.01 A to a maximal value of 2.6 A, and thereafter, it is decreased back to zero. Each current value is held for 10–20 s until the MF takes its equilibrium shape. Thus, the process of the MF transformation can be seen as quasi-static. The following values of V_0 are selected: 0.4 cm^3, 0.8 cm^3 and 2 cm^3.

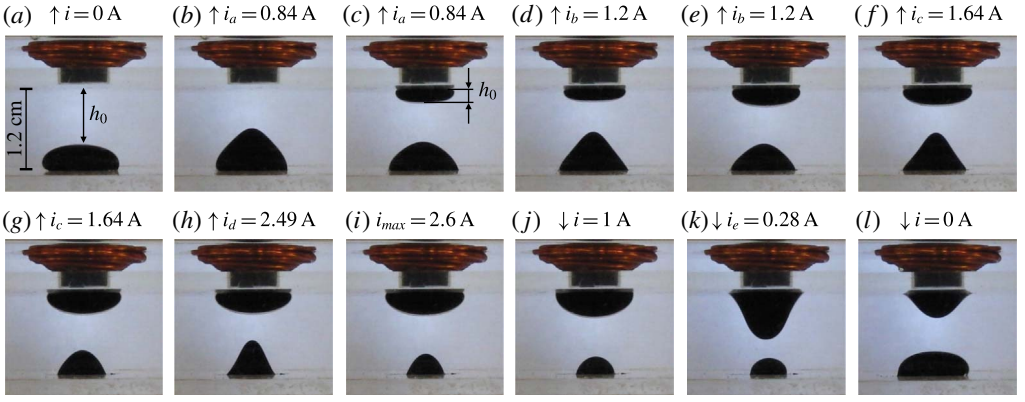

FIGURE 2. (Colour online) Equilibrium surface shapes of an MF volume $V_0 = 0.4$ cm^3. Panels (*a–i*) correspond to the increasing current i from 0 A to 2.6 A, whereas (*i–l*) conform to the decreasing current i from 2.6 A to 0 A.

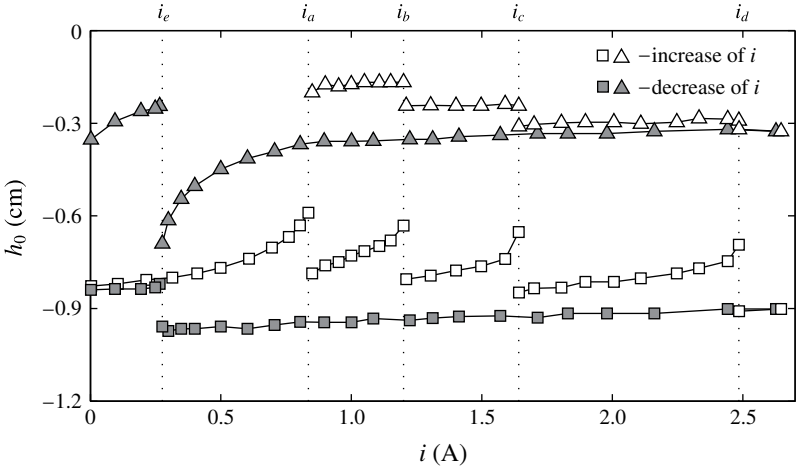

FIGURE 3. Dependence of h_0 on i for $V_0 = 0.4$ cm^3: □ – drop on the lower plate; △ – drop on the upper plate. Current values at which abrupt changes occur: $\uparrow i_a = 0.84$ A, $\uparrow i_b = 1.2$ A, $\uparrow i_c = 1.64$ A, $\uparrow i_d = 2.49$ A and $\downarrow i_e = 0.28$ A.

During experimental series with various MF volumes, it is shown that three different simply connected axisymmetric forms of the volume may exist, namely: a drop on the lower plate, a drop retained on the upper plate beneath the coil or an MFB between the plates. Their equilibrium surface shape may be described by a function $z = h(r)$. A set of solutions split into two disconnected parts of drops on the lower and upper plates with the total MF volume is also possible.

As a characteristic parameter of the drops on the upper and lower plates, the coordinate $h_0 = h(0)$, $-d \leqslant h_0 \leqslant 0$, of the intersection point of the MF surface $z = h(r)$ with the z axis is chosen, see figure 2(*a*,*c*). The MFB is characterised by the radius $r_0 > 0$ of the contact spot of the MF with the upper plate: $h(r_0) = 0$, see figure 4(*e*). These coordinates are measured on the experimental photos and plotted against the current.

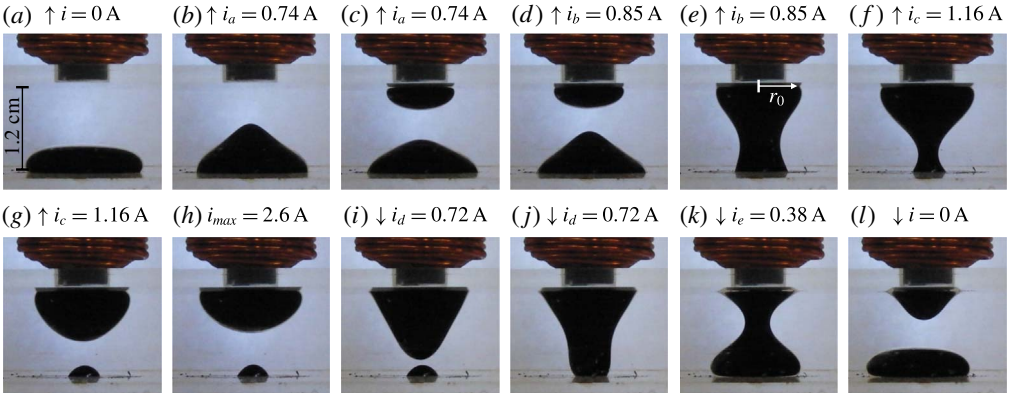

FIGURE 4. (Colour online) Equilibrium surface shapes of an MF volume $V_0 = 0.8$ cm^3. Panels (*a–h*) correspond to the increasing current i from 0 A to 2.6 A, whereas (*h–l*) conform to the decreasing current i from 2.6 A to 0 A.

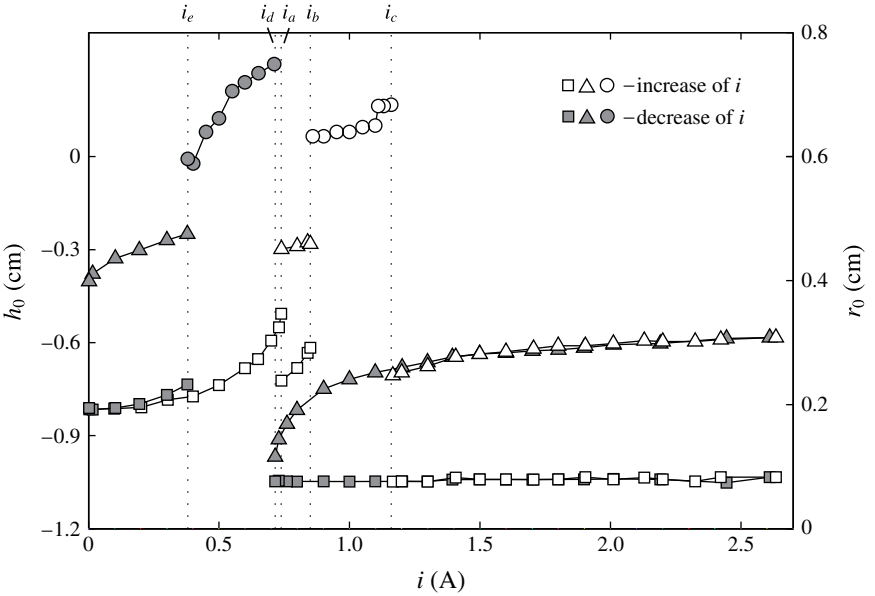

FIGURE 5. Dependencies of h_0 (left axis) and r_0 (right axis) on i for $V_0 = 0.8$ cm^3: □ – h_0 for the drop on the lower plate; △ – h_0 for the drop on the upper plate; ○ – r_0 for the MFB. Current values at which abrupt changes occur: $\uparrow i_a = 0.74$ A, $\uparrow i_b = 0.85$ A, $\uparrow i_c = 1.16$ A, $\downarrow i_d = 0.72$ A and $\downarrow i_e = 0.38$ A.

For a MF volume of $V_0 = 0.4$ cm^3, several stepwise changes in the MF surface shape take place when the current either increases or decreases quasi-statically from 0 A to 2.6 A, see figure 2. At four critical values of the increasing current i, namely $i_a = 0.84$ A, $i_b = 1.2$ A, $i_c = 1.64$ A and $i_d = 2.49$ A, the drop of the MF on the lower plate becomes unstable, a part of it jumps suddenly up and initially forms, and subsequently merges with, a drop on the upper plate. The first such transition at $\uparrow i_a = 0.84$ A is shown in figure 2(*b*,*c*), the second one occurring at $\uparrow i_b = 1.2$ A in figure 2(*d*,*e*), etc. This is because, when the current reaches these critical values, the

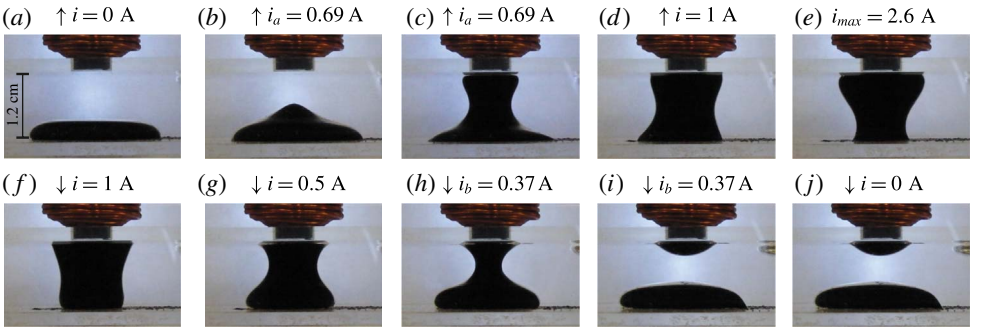

FIGURE 6. (Colour online) Equilibrium surface shapes of an MF volume $V_0 = 2$ cm^3. Panels (*a–e*) correspond to the increasing current i from 0 A to 2.6 A, whereas (*e–j*) conform to the decreasing current i from 2.6 A to 0 A.

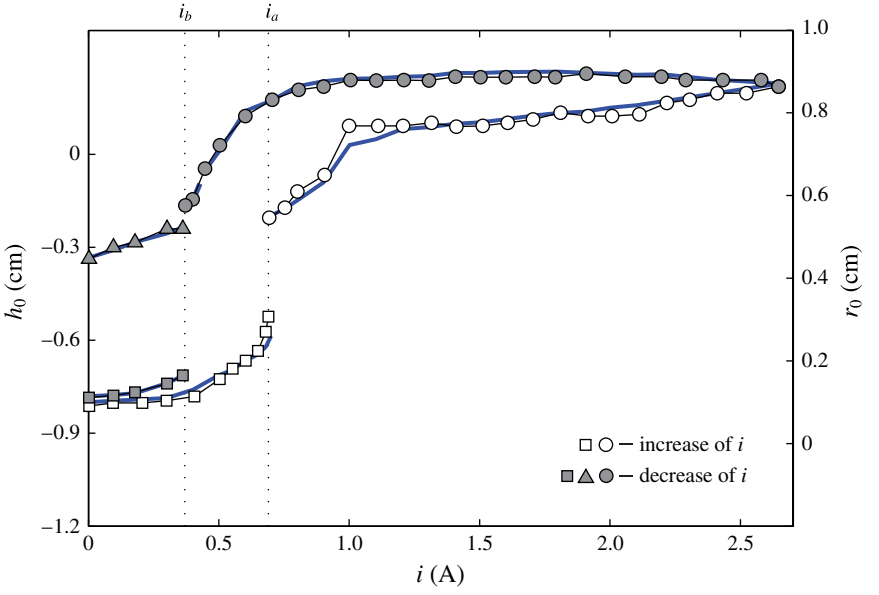

FIGURE 7. (Colour online) Dependencies of h_0 (left axis) and r_0 (right axis) on i for $V_0 = 2$ cm^3. Measured data: □ – h_0 for the drop on the lower plate; △ – h_0 for the drop on the upper plate; ○ – r_0 for the MFB. Current values at which abrupt changes occur: $\uparrow i_a = 0.69$ A and $\downarrow i_b = 0.37$ A. Theoretical result is shown by the solid line.

imbalance between gravitational, surface and magnetic energies occurs for the present volume of the drop on the lower plate. Note that, in general, the number of such transitions depends on the pattern of the current change and the dynamics of the process. However, in the described experiment, the current is changed in a quasi-static manner, and so these four transitions and their critical currents are most likely stable from the point of reproducibility. For each jump, the volume of the MF transferred from one plate to the other can be approximated by image analysis of experimental photos.

At $i_{max} = 2.6$ A almost the whole initial volume gathers into a drop on the upper plate, only a small droplet is left on the lower plate, see figure 2(*i*). When the current

decreases, these two drops retain up to a value $\downarrow i_e = 0.28$ A, at which a part of the upper drop separates and falls abruptly onto the lower plate. At the end of the process, when $i = 0$ A, the initial simply connected MF volume consists of two separate drops, see figure 2(*a*,*l*). It should be noted that no MFB of $V_0 = 0.4$ cm^3 between the plates was observed for any values of the increasing and decreasing current. The dependence of h_0 on i for $V_0 = 0.4$ cm^3 is shown in figure 3. Hereinafter, the white and grey markers correspond to the increasing and decreasing current, respectively. This graphic clearly shows that there is a hysteresis phenomenon of the MF surface shape.

Figure 4 shows equilibrium surface shapes of an MF volume $V_0 = 0.8$ cm^3. In this case, the formation of the MFB occurs both for the increasing and decreasing current. As the current increases from $i = 0$ A, the initial volume on the lower plate rises and becomes unstable at $\uparrow i_a = 0.74$ A as it divides into two drops, see figure 4(*b*,*c*). At the next threshold value, $\uparrow i_b = 0.85$ A, the upper and lower drops gather into an MFB (figure 4*d*,*e*), which at $\uparrow i_c = 1.16$ A breaks up into two drops (figure 4*f*,*g*). These resulting drops remain with the increase in current to $i_{max} = 2.6$ A and its further decrease down to $\downarrow i_d = 0.72$ A. At this critical value, the MFB between the plates occurs again from the coalescence of the upper and lower drops, see figure 4(*i*,*j*). It exists for the current from $\downarrow i_d = 0.72$ A to $\downarrow i_e = 0.38$ A and then disintegrates into two drops again. So, the MFB may occur in completely different ranges of the increasing and decreasing current. The dependencies of the coordinates h_0 and r_0 of the observed surface shapes of $V_0 = 0.8$ cm^3 are plotted against the current i in figure 5.

For the MF volume $V_0 = 2$ cm^3 equilibrium surface shapes are shown in figure 6. With the increase in current from $i = 0$ A, the initial drop on the lower plate becomes unstable at $\uparrow i_a = 0.69$ A and transforms abruptly to an MFB between the plates, see figure 6(*b*,*c*). The resulting bridge between the plates exists up till the value $i_{max} = 2.6$ A. Then, for the decreasing current the MFB remains up to $\downarrow i_b = 0.37$ A and disintegrates into two drops, as for all other described cases (figure 6*h*,*i*). The dependencies of h_0 and r_0 on i are presented in figure 7.

To summarise, in the experimental series with various MF volumes and a fixed distance between the plates, the abrupt behaviour and hysteresis of the surface shape are studied as the current changes quasi-statically. The current values at which these abrupt transformations take place are determined. Moreover, the wetting hysteresis phenomenon is observed, that is the difference between the contact angle values for the increasing and decreasing current. To take this effect into account in further numerical calculations of an MF equilibrium shape, the contact angles θ_0 on the upper and lower plates are measured through image analysis of experimental photos. In the case of $V_0 = 2$ cm^3, these dependencies $\theta_0(i)$ will be given in § 4.3. As a result, the MF equilibrium shape exhibits two types of hysteresis when the current changes cyclically. First, there is a bistability of simply connected shapes in certain ranges of currents (e.g. figure 7 at $i = 0.5$ A), and it depends on the initial conditions and pattern of the current change as to which one is observed. Second, due to the contact angle hysteresis, the MF volume can have different surface forms, see figure 6(*d*,*f*) at $i = 1$ A.

2.3. *Disintegration of the MFB between the plates*

The realisation of an MFB depends mainly on the current and the relation of the MF volume to the distance between the plates. To determine ranges of parameters for which the MFB exists, the following experiment has been carried out. At a certain

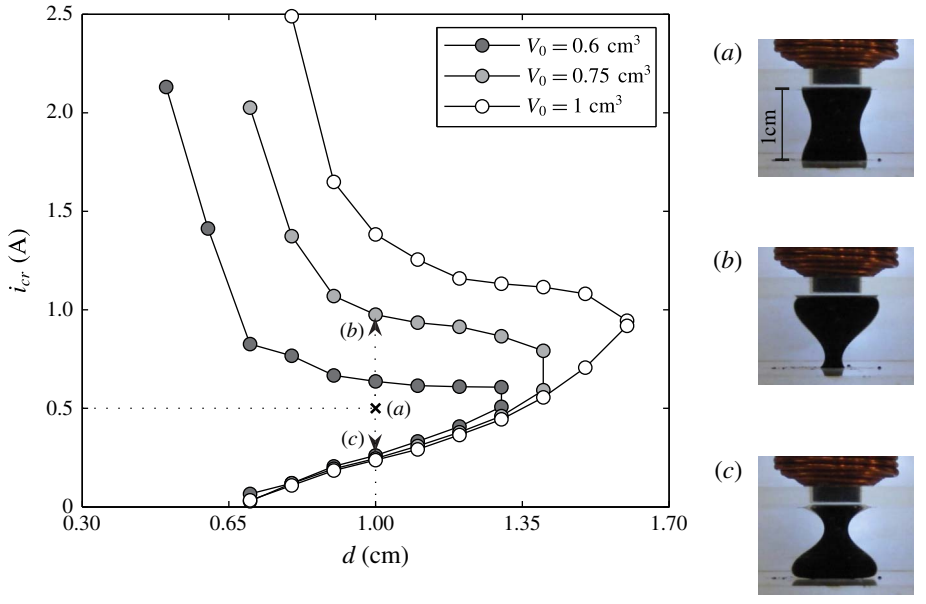

FIGURE 8. (Colour online) Stability curves $i_{cr} = i_{cr}(d)$ of the MFB of $V_0 = 0.6$ cm^3, 0.75 cm^3 and 1 cm^3. Surface shapes of the MFB for $V_0 = 0.75$ cm^3 and $d = 1$ cm: (*a*) $i = 0.5$ A; (*b*) $\uparrow i_{cr} = 0.98$ A; (*c*) $\downarrow i_{cr} = 0.25$ A.

value of the current $i > 0$ A, an MF volume is injected so that it takes a form of the axisymmetric MFB. The distance d between the horizontal plates is fixed. In the first attempt, the current in the coil increases quasi-statically and decreases in the second one. In both cases, critical current values $i_{cr} = i_{cr}(d)$ at which the MFB breaks abruptly into two drops are measured.

The experiments were carried out for three different MF volumes V_0: 0.6 cm^3, 0.75 cm^3 and 1 cm^3. The distance between the plates was changed in the range from 0.5 cm to 1.6 cm with a step size 1 mm. The dependencies of the critical current $i_{cr} = i_{cr}(d)$ are presented in figure 8. One can see that these lines have the same qualitative character. For each value V_0, the dependence $i_{cr} = i_{cr}(d)$ is the so-called stability curve of the MFB between the plates. Since the curve divides the plane of parameters i and d into two parts, the region to the left of it corresponds to the values, for which a stable MFB can exist, see figure 8(*a*). On the contrary, for the values of i and d from the right part of the plane the MFB cannot be created and does not exist at all.

3. Theoretical analysis of an MF equilibrium shape based on the variational method

3.1. *Formulation of the problem*

Consider a heavy incompressible MF and a surrounding NML lying between horizontal plates, which are fixed at a distance d from each other, in the presence of a non-uniform magnetic field. In the axisymmetric case, all parameters are assumed to depend on the cylindrical coordinates r and z, see figure 1. As shown in § 2.2, a given MF volume V_0 may take three different simply connected axisymmetric forms, namely: a drop on the lower plate, a drop on the upper plate or an MFB. Consider

that the curve $z = h(r)$ determines the equilibrium surface shape of the interface between the MF drop on the lower (or upper) plate and the NML. For the MFB between the plates, it is convenient to describe its axisymmetric surface shape with a function $r = \zeta(z)$.

For the theoretical considerations, the non-inductive approximation is assumed, that is, the MF is weakly magnetisable so that it does not distort the strength $\boldsymbol{H}$ of an applied magnetic field. The subscripts 1 and 2 denote the parameters of the MF and the NML, respectively.

The energy of a finite MF volume surrounded by an NML consists of the surface energy, the energy in the gravity field and the magnetostatic energy (Landau & Lifshitz 1980):

$$F = \int_S \sigma \, \mathrm{d}s + (\rho_1 - \rho_2) g \int_V (z + d) \, \mathrm{d}v - \int_V \int_0^{H(r,z)} M_1(H) \, \mathrm{d}H \, \mathrm{d}v. \tag{3.1}$$

Here, $\sigma = \text{const.}$ is the surface tension coefficient, $\mathrm{d}s$ is the element of the interface S, ρ_1 and ρ_2 are the densities of the MF and NML, wherein $\rho_1 > \rho_2$, g is the gravity acceleration, $\mathrm{d}v$ is the element of the MF volume V and $H(r, z)$ is the strength of the axisymmetric magnetic field.

The magnetisation of the MF $M_1(H)$ with a small concentration of ferromagnetic particles can be described by the Langevin formula

$$M_1(\xi) = M_{1S} \left(\coth \xi - \frac{1}{\xi} \right), \quad \xi = \frac{mH}{kT}, \quad m = \frac{M_{1S}}{n}. \tag{3.2a–c}$$

Here, $T = \text{const.}$ is the temperature of the fluids, k is the Boltzmann constant and M_{1S} is the MF saturation magnetisation, which is linked with the magnetic moment m of a single ferromagnetic particle and the number of ferromagnetic particles n.

The MF energy F described by formula (3.1) is a nonlinear functional defined on the class of continuously differentiable functions $z = h(r)$ (or $r = \zeta(z)$ for the MFB) with variable end points. In the static equilibrium state, the energy F must have minimum for all surface shape variations satisfying the condition of the constant MF volume:

$$V_0 = \int_V \mathrm{d}v = \text{const.} \tag{3.3}$$

3.2. *Variation of the energy functional*

In what follows, without loss of generality, we will only consider the variation of the functional F for the simply connected MF drop on the lower plate. For the drop on the upper plate and the MFB, the analysis procedure is the same, with the differences given in appendices A and B, respectively.

The energy functional $F[h]$ of the drop on the lower plate with the surface $z = h(r)$ can be calculated by formula (3.1) accounting for (3.2)

$$\begin{aligned} F[h] \;=\; & 2\pi \int_0^{r_1} \left(\sigma r \sqrt{1 + h'^2(r)} - (\sigma_{s2} - \sigma_{s1}) r + \frac{1}{2} r g (\rho_1 - \rho_2)(h(r) + d)^2 \right. \\ & \left. - nkT \int_{-d}^{h(r)} r \ln \frac{\sinh(mH(r, z)/(kT))}{mH(r, z)/(kT)} \, \mathrm{d}z \right) \mathrm{d}r. \end{aligned} \tag{3.4}$$

Here, $(r_1, -d)$, $r_1 > 0$, is the point of intersection of the surface $z = h(r)$ with the lower plate, a prime denotes the derivative with respect to r. The surface tension forces $\sigma = \sigma_{12}$, σ_{s1} and σ_{s2} act between the phases, where the subscripts 1, 2 and s correspond to the MF, NML and the solid plate, respectively. In accordance with the Young equation, they are linked by the relation $\sigma \cos\theta_0 = \sigma_{s2} - \sigma_{s1}$, where θ_0 is the contact angle, $0 \leqslant \theta_0 \leqslant \pi$.

According to the Euler theorem in the calculus of variations, to find the minimum of the energy functional (3.4) the following auxiliary functional $\Psi[h]$ is considered:

$$\Psi[h] = F[h] - p_0 V_0[h] = 2\pi \int_0^{r_1} f(r, h, h')\,\mathrm{d}r, \quad V_0[h] = 2\pi \int_0^{r_1} r(h(r) + d)\,\mathrm{d}r, \quad (3.5a,b)$$

where p_0 is a constant to be determined. The forms of Ψ in the case of the drop on the upper plate and the MFB are given in appendices A and B, respectively.

The functional $\Psi[h]$ is defined by (3.5) in the class of continuously differentiable functions $z = h(r)$ with variable end points $(0, h_0)$ and $(r_1, -d)$. Here, h_0, $-d < h_0 < 0$, and $r_1 > 0$ are unknown coordinates to be determined.

Let $u(r)$ be a certain variation of the drop surface shape $z = h(r)$ in the plane $\phi = \text{const}$. End points of the variable curve $h(r) + u(r)$ are denoted by $(0, h_0 + \delta h_0)$ and $(r_1 + \delta r_1, d)$. The variation $\delta\Psi[u]$ of the functional $\Psi[h]$ is defined as an expression, which is linear in increments $u(r)$, $u'(r)$, δh_0, δr_1 and which differs from the total increment $\Psi[h + u] - \Psi[h]$ by a quantity higher by more than an order of magnitude as compared to the distance between the functions $h(r)$ and $h(r) + u(r)$ (Gelfand & Fomin 2000):

$$\frac{1}{2\pi}\delta\Psi[u] = \int_0^{r_1} \left(f'_h - \frac{\mathrm{d}}{\mathrm{d}r} f'_{h'}\right) u(r)\,\mathrm{d}r + (f - h' f'_{h'})\Big|_{r=r_1} \delta r_1 - f'_{h'}|_{r=0}\delta h_0, \qquad (3.6)$$

where the prime and the subscripts h and h' denote partial derivatives with respect to the corresponding arguments.

In order for the energy functional $F[h]$ extremum to be reached on the curve $h(r)$, it is necessary that the variation $\delta\Psi[u]$ vanishes for $z = h(r)$ and all admissible $u(r)$ (Gelfand & Fomin 2000). From the requirement that the integrand in (3.6) be equal to zero, in view of (3.4) and (3.5), we have the following Euler–Lagrange equation

$$p_0 - g(\rho_1 - \rho_2)(h(r) + d) + nkT \ln \frac{\sinh(mH(r, h(r))/(kT))}{mH(r, h(r))/(kT)} = -\sigma \frac{h''(r) + h'^3(r)/r + h'(r)/r}{(1 + h'^2(r))^{3/2}}. \qquad (3.7)$$

Since $u(r)$ is an arbitrary function, the terms in front of the independent increments δh_0 and δr_1 in (3.6) should be zero. Therefore, the following boundary conditions at the variable end points of the admissible curve $z = h(r)$ must be satisfied:

$$\left.\begin{array}{ll} h(0) = h_0, & h'(0) = 0, \quad \text{for } -d < h_0 < 0, \\ h(r_1) = -d, & h'(r_1) = -\tan\theta_0, \quad \text{for } r_1 > 0. \end{array}\right\} \qquad (3.8)$$

Thus, to find the minimum of the functional $F[h]$ on the curve $z = h(r)$ with variable end points, it is required first to solve the Euler–Lagrange equation (3.7). It is a nonlinear second-order differential equation for the curve $h(r)$, which determines the

axisymmetric surface shape of the MF drop on the lower plane. Then, the values of two arbitrary constants appearing in the general solution of (3.7), the constant p_0, and the coordinates h_0 and r_1 of the variable end points, are determined from the boundary conditions (3.8) and the condition $V_0 = \text{const}$.

It can be shown that (3.7) also determines the surface shape of the MF drop on the upper plate with one correction, with the requirement of replacing the minus by a plus on the right-hand side of the equation. Then, the boundary conditions at the variable end points are: $h(0) = h_0$, $h'(0) = 0$, and $h(r_1) = 0$, $h'(r_1) = \tan\theta_0$ with $-d < h_0 < 0$ and $r_1 > 0$.

In order to determine the shape $r = \zeta(z)$ of the MFB between the plates, the Euler–Lagrange equation $f'_{\zeta} - (\mathrm{d}/\mathrm{d}z)f'_{\zeta'} = 0$ should be solved with the corresponding form of the function $f(z, \zeta, \zeta')$ given in appendix B. In this case, the boundary conditions are $\zeta(0) = r_0$, $\zeta'(0) = \cot\theta_0$, and $\zeta(-d) = r_1$, $\zeta'(-d) = -\cot\theta_0$, where $r_0, r_1 > 0$ are variable coordinates to be determined.

It should be noted that the solutions of the Euler–Lagrange equation do not always realise a local minimum or maximum of the MF energy since this equation gives only a necessary condition for the functional to have an extremum.

3.3. *Sufficient conditions of the minimum energy*

To find sufficient conditions for a functional minimum, it is necessary to introduce a new concept, namely, the second variation of a functional. Denote by $\delta^2\Psi[u]$ the terms of the second order relative to the end variations δh_0 and δr_1, the increment of $u(r)$ and its derivative, which are determined by the expansion of $\Psi[h+u] - \Psi[h]$ in a Taylor series. The expression $\delta^2\Psi[u]$ is a quadratic functional and is called the second variation of the functional $\Psi[h]$.

In order that the minimum of the energy functional $F[h]$ together with the subsidiary condition of the constancy of the volume $V_0[h]$ be reached on the curve $z = h(r)$, it is necessary and sufficient that on the extremal $z = h(r)$ the differential $\delta\Psi[u]$ be equal to zero and the second variation $\delta^2\Psi[u]$ be positive definite for all admissible surface perturbations $u(r)$:

$$\delta\Psi[u] \equiv 0, \quad \delta^2\Psi[u] > 0 \quad \text{for } z = h(r). \tag{3.9a,b}$$

Accounting for formula (3.4) and the boundary conditions (3.8) and $f''_{hh'} = 0$, the expression for the second variation of the drop on the lower plate takes the following form:

$$\frac{1}{2\pi}\delta^2\Psi[u] = (f'_r - h'f'_h)|_{r=r_1}\delta r_1^2 + \int_0^{r_1} (f''_{h'h'}u'^2 + f''_{hh}u^2)\,\mathrm{d}r. \tag{3.10}$$

Notice that $f''_{h'h'} = \sigma r(1+h'^2)^{-3/2} > 0$ for $r > 0$.

Let us introduce two continuously differentiable functions $\omega_1(r)$ and $\omega_2(r)$, which are the solutions of the following equation

$$f''_{h'h'}(f''_{hh} + \omega'(r)) = \omega^2(r), \tag{3.11}$$

and satisfy the respective boundary conditions

$$\omega_1(0) = 0 \quad \text{and} \quad \omega_2(r_1) = \left(\frac{f'_r}{h'^2} - \frac{f'_h}{h'}\right)\bigg|_{r=r_1}. \tag{3.12a,b}$$

The sufficient condition for the second variation $\delta^2\Psi[u]$ to be positive definite for all admissible variations $u(r)$ is that the functions $\omega_1(r)$ and $\omega_2(r)$ fulfil the condition $\omega_2 - \omega_1 > 0$ for any point of the segment $[0, r_1]$.

This is due to the fact that, in this case, the following transformation of $\delta^2\Psi[u]$ can be made. Divide the integral in (3.10) into two parts: from 0 to r_* and from r_* to r_1, where $0 < r_* < r_1$. Then, we add to and subtract from each integrand a term of the form $\mathrm{d}(\omega_i u^2)$, $i = 1, 2$. According to (3.11), the reformed integrands are both perfect squares. In view of $u(0) = \delta h_0$ and $u(r_1) = -h'(r_1)\delta r_1$, the expression (3.10) for $\delta^2\Psi[u]$ is simplified to

$$\frac{1}{2\pi}\delta^2\Psi[u] = \omega_1(0)\delta h_0^2 + (f'_r - h'f'_h - \omega_2 h'^2)|_{r=r_1}\delta r_1^2 + (\omega_2 - \omega_1)|_{r=r_*}u^2(r_*) + \int_0^{r_*} f''_{h'h'}\left(u' + \frac{\omega_1}{f''_{h'h'}}u\right)^2 \mathrm{d}r + \int_{r_*}^{r_1} f''_{h'h'}\left(u' + \frac{\omega_2}{f''_{h'h'}}u\right)^2 \mathrm{d}r > 0. \quad (3.13)$$

Since the first two terms are zero according to (3.12), it is obvious that if $\omega_2 - \omega_1 > 0$ on $[0, r_1]$, the second variation $\delta^2\Psi[u]$ will be positive definite for all admissible $u(r)$. This is the sufficient condition for the minimum of the energy functional defined on the class of axisymmetric continuously differentiable functions $z = h(r)$ describing the MF equilibrium surface shape.

For the MF drop on the lower plate (3.11) and conditions (3.12) have the following forms:

$$\frac{\mathrm{d}\omega(r)}{\mathrm{d}r} = \frac{(1 + h'^2(r))^{3/2}}{\sigma r}\omega^2(r) - (\rho_1 - \rho_2)gr + \frac{nkTr}{H(r, h(r))}\left(\frac{\partial H(r, z)}{\partial z}\right)\Big|_{z=h(r)}\left(\frac{mH(r, h(r))}{kT}\coth\left(\frac{mH(r, h(r))}{kT}\right) - 1\right), \quad (3.14)$$

$$\omega_1(0) = 0, \quad \omega_2(r_1) = \sigma\cos\theta_0 - \frac{r_1}{\tan\theta_0}\left(p_0 + nkT\ln\frac{\sinh(mH(r_1, -d)/(kT))}{mH(r_1, -d)/(kT)}\right) \quad (3.15a,b)$$

Equation (3.14) can be solved numerically taking into account that the shape of the MF surface $z = h(r)$ is determined by (3.7).

The analysis of the minimum energy problem for the MF drop on the upper plate is similar to the case above. The characteristic ω functions are defined by the same equation (3.11) with the boundary conditions (3.12) taking into account the corresponding form of the function $f(r, h, h')$ given in appendix A. The sufficient condition of the minimum energy is identical: $\omega_2 - \omega_1 > 0$ on $[0, r_1]$, where r_1 is determined by $h(r_1) = 0$.

For the MFB between the plates with the axisymmetric surface shape $r = \zeta(z)$, the sufficient condition of the minimum energy is $\omega_2 - \omega_1 > 0$ on $[-d, 0]$. The equation for the determination of the functions $\omega_i(z)$, $i = 1, 2$ and their boundary conditions are given in appendix B.

3.4. *Necessity and sufficiency of the minimum conditions*

Consider the case where the sufficient conditions of the minimum energy are not satisfied for an extremal solution $z = h(r)$ of the MF surface shape. Then, it may be shown that there exists another continuously differentiable function in the weak

neighbourhood of $h(r)$, which provides a smaller value for the energy functional than the extremal $h(r)$. This will reveal that the curve $z = h(r)$ cannot realise a local minimum for the energy functional.

Let us suppose that the characteristic ω functions are defined on the whole segment $[0, r_1]$, but $\omega_2 - \omega_1 < 0$. Using the substitution $\omega = -f''_{h'h'}u'/u$, we may introduce two perturbation functions $u_1(r)$ and $u_2(r)$ on $[0, r_1]$:

$$u_1(r) = \delta h_0 \mathrm{e}^{-\int_0^r (\omega_1(t)/f''_{h'h'}(t))\,\mathrm{d}t}, \quad u_2(r) = -h'(r_1)\delta r_1 \mathrm{e}^{\int_r^{r_1} (\omega_2(t)/f''_{h'h'}(t))\,\mathrm{d}t}. \tag{3.16a,b}$$

Note that these functions are the solutions of (3.11) written in the form: $(f''_{h'h'}u'(r))' = f''_{hh}u(r)$. They satisfy the following boundary conditions: $u_1(0) = \delta h_0$, $u'_1(0) = 0$ and $u_2(r_1) = -h'(r_1)\delta r_1$, $u'_2(r_1) = (\omega_2 h'/f''_{h'h'})|_{r=r_1}\delta r_1$. So, it is possible to define them on the whole segment $[0, r_1]$, even when the functions ω_1 and ω_2 do not exist everywhere on it. Moreover, it can be shown that the expression $f''_{h'h'}(u'_1u_2 - u_1u'_2) = C$ is constant for $0 < r \leqslant r_1$. This means that the difference $\omega_2 - \omega_1$ does not change sign within the common domain of these functions.

Let $r = r_*$ be a point of the segment $[0, r_1]$. Assuming the end point variations δh_0 and δr_1 are small and linked so that $u_1(r_*) = u_2(r_*)$, the piecewise differentiable perturbation $\hat{u}(r)$ is defined as $\hat{u}(r) = u_1(r)$ for $0 \leqslant r \leqslant r_*$ and $\hat{u}(r) = u_2(r)$ for $r_* \leqslant r \leqslant r_1$. Using (3.12), (3.13) and (3.16), it is possible to show that in the weak neighbourhood of $h(r)$ the functional value for the curve $h + \hat{u}$ is smaller than $\Psi[h]$:

$$\Psi[h + \hat{u}] - \Psi[h] = \tfrac{1}{2}\delta^2\Psi[\hat{u}] = \pi(\omega_2 - \omega_1)|_{r=r_*}\hat{u}^2(r_*) = \pi C < 0. \tag{3.17}$$

We can now construct a continuously differentiable perturbation $u(r)$ on $[0, r_1]$ so that the difference $\Psi[h + u] - \Psi[h + \hat{u}]$ is infinitesimally small. For any $\varepsilon > 0$, consider an ε neighbourhood of the point $r = r_*$, where the derivative $\hat{u}'$ has a jump discontinuity, since $u'_1(r_*) \neq u'_2(r_*)$. The smooth curve $u(r)$ is derived from $\hat{u}(r)$ by replacing the part in the interval $[r_* - \varepsilon, r_* + \varepsilon]$. For this, let us join the points $\hat{u}'(r_* - \varepsilon)$ and $\hat{u}'(r_* + \varepsilon)$ by a continuous curve $\upsilon(r)$ in such a way that

$$\int_{r_*-\varepsilon}^{r_*+\varepsilon} \upsilon(r)\,\mathrm{d}r = \int_{r_*-\varepsilon}^{r_*} u'_1(r)\,\mathrm{d}r + \int_{r_*}^{r_*+\varepsilon} u'_2(r)\,\mathrm{d}r. \tag{3.18}$$

Therefore, we may define $u(r)$ as follows:

$$u(r) = \begin{cases} u_1(r), & \text{for } 0 \leqslant r \leqslant r_* - \varepsilon, \\ u_1(r_* - \varepsilon) + \displaystyle\int_{r_*-\varepsilon}^{r} \upsilon(t)\,\mathrm{d}t, & \text{for } |r - r_*| \leqslant \varepsilon, \\ u_2(r), & \text{for } r_* + \varepsilon \leqslant r \leqslant r_1. \end{cases} \tag{3.19}$$

It is easy to verify that the function $u(r)$ is continuously differentiable on $[0, r_1]$ and satisfies the boundary conditions $u(0) = \delta h_0$ and $u(r_1) = -h'(r_1)\delta r_1$. At the points $r = r_* \pm \varepsilon$, we have $u = \hat{u}$ and $u' = \hat{u}'$.

Considering (3.5), the difference between the functional values on the curves $h + u$ and $h + \hat{u}$ may be simplified as:

$$\Psi[h + u] - \Psi[h + \hat{u}] = 2\pi \int_{r_*-\varepsilon}^{r_*+\varepsilon} (f(r, h + u, h' + u') - f(r, h + \hat{u}, h' + \hat{u}'))\,\mathrm{d}r = O(\varepsilon). \tag{3.20}$$

If ε is sufficiently small, the curve $h + u$ lies in the weak neighbourhood of $h(r)$. So, for an appropriate choice of ε and according to (3.17), the difference $\Psi[h + u] - \Psi[h]$

can be made negative:

$$\Psi[h+u]-\Psi[h]=\pi C+O(\varepsilon)<0. \tag{3.21}$$

Hence, if the conditions of the minimum energy are not satisfied, the admissible surface perturbation $u(r)$ defined by (3.19) is found such that the functional value $\Psi[h+u]$ is smaller than $\Psi[h]$. This means that on the extremal solution $z=h(r)$, the local minimum of the energy functional cannot be reached. In other words, the surface shape $z=h(r)$ is unstable.

Without going into the details, it should be noted that the reasoning will be the same also in the case where the characteristic functions $\omega_1(r)$ and $\omega_2(r)$ are not defined on the whole segment $[0, r_1]$, and even where they do not have a common domain. Anyway, it is possible to choose the point $r=r_*$ so that the expression (3.17) is negative.

To summarise, the condition $\omega_2-\omega_1>0$ on the whole segment $[0, r_1]$ (or $[-d, 0]$) is necessary and sufficient for a local minimum of the energy functional to be reached on the curve $z=h(r)$ (or $r=\zeta(z)$). The proposed theoretical method makes is possible for the given parameters of the problem to calculate an MF equilibrium surface shape and examine its stability relative to small axisymmetric surface perturbations.

4. Numerical calculation of an MF equilibrium shape and its stability analysis

In this section, the results of numerical calculations of the equilibrium surface shape of an MF volume are presented. The stability of the obtained solutions is analysed using the theoretically derived necessary and sufficient conditions. The section is organised as follows: § 4.1 shows the geometry of the magnetic field imposed by the electromagnet used in the experiment. As we show, the wetting hysteresis phenomenon occurs in the experiment when the current in the coil is changed cyclically, e.g. see figure 6(*d*,*f*). That is why, first, the results in § 4.2 are carried out assuming that the contact angle at the MF–NML–solid plate interface is constant and equals $\theta_0=80°$. For this particular value, a variety of solutions for the simply connected MF surface shapes of the given volume is shown. Then in § 4.3, the results are obtained taking into account the wetting hysteresis phenomenon, i.e. considering the dependencies of the contact angle $\theta_0(i)$ on the current. Thereby, the comparison between numerically computed and experimentally observed MF surface shapes is made.

Numerical calculations are carried out using MATLAB®. A second-order differential equation that describes the MF surface shape (in particular, (3.7) for the drop on the lower plate) is first reduced to the system of three nonlinear first-order differential equations by introducing the natural parametrisation of the curve $z=h(r)$. The material properties are defined according to the parameters used in the experiment, see § 2.1 and table 1. The other parameters that enter the calculation are $g=980$ cm s^{-2}, $T=300$ K, $k=1.38\times10^{-16}$ erg K^{-1}, $n=3.82\times10^{16}$ cm^{-3}.

4.1. *Modelling of the stationary magnetic field of the electromagnetic coil*

When solving numerically, e.g. (3.7) and (3.14) for the drop on the lower plate, the problem of magnetic field distribution $H(r, z)$ in the area between the horizontal plates of the set-up occurs. The modelling and the calculation of the stationary magnetic field $H(r, z)$ of the axisymmetric electromagnetic coil with the inserted ferrite core were done numerically using a finite element software package (ANSYS®). The geometry and material properties of the model were defined according to the parameters of the coil and the core used in the experiment, see § 2.1. For numerical computation,

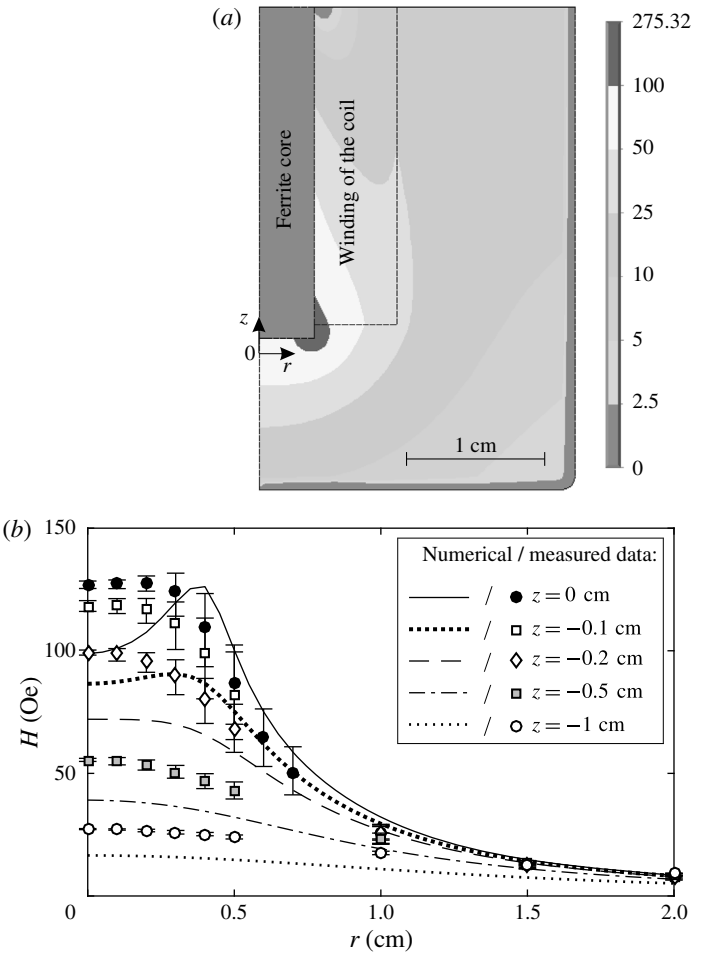

FIGURE 9. (*a*) Magnetic field distribution $H(r, z)$ (in Oe) of the electromagnetic coil with the ferrite core used in the experiment for $i = 0.5$ A; (*b*) comparison between numerical and measured values of $H(r, z)$ for $i = 0.5$ A.

the PLANE53 element was chosen, which allows two-dimensional modelling of the magnetic field in axisymmetric problems. Far-field elements are defined by INFIN110 element type. The domain is meshed with elements of 0.05 cm edge length. Figure 9(*a*) shows the distribution of the magnetic field strength $H(r, z)$ in the vicinity of the lower end of the core obtained numerically. The results are compared with the data measured for the experimental coil with an analogue Hall sensor, see figure 9(*b*). The discrepancy in the results may be caused by the singularity of the magnetic field at the edge of the core and the real geometrical dimensions of the Hall sensor surface.

4.2. *Stability of the equilibrium surface shape of MF drops and MFB for a constant contact angle*

In this part, the numerical calculations are carried out assuming a constant contact angle of $\theta_0 = 80°$ at the MF–NML–solid plate interface. Therefore, the obtained results can be compared only qualitatively with experimental results of § 2.

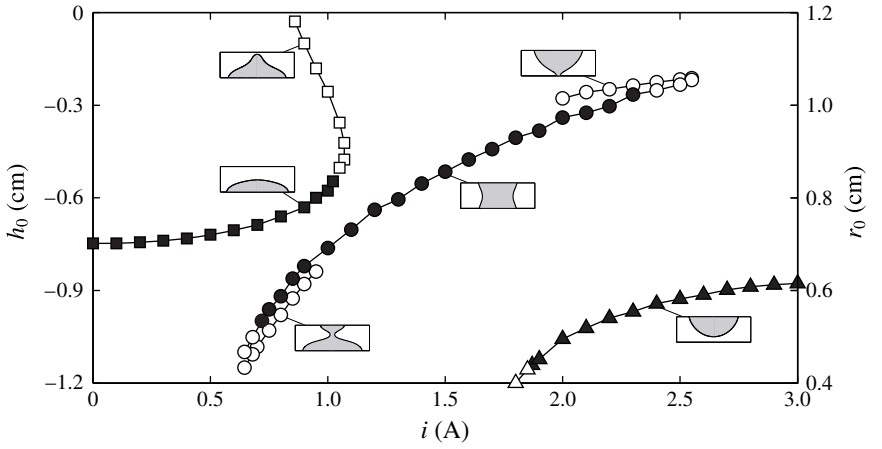

FIGURE 10. Dependencies of h_0 (left axis) and r_0 (right axis) on i obtained numerically in the case of a constant contact angle $\theta_0 = 80°$ for $V_0 = 2$ cm^3 and $d = 1.2$ cm: □ – h_0 for the drop on the lower plate; △ – h_0 for the drop on the upper plate; ○ – r_0 for the MFB. Stable solutions, on which the local minimum of the energy functional is reached are shown by black symbols.

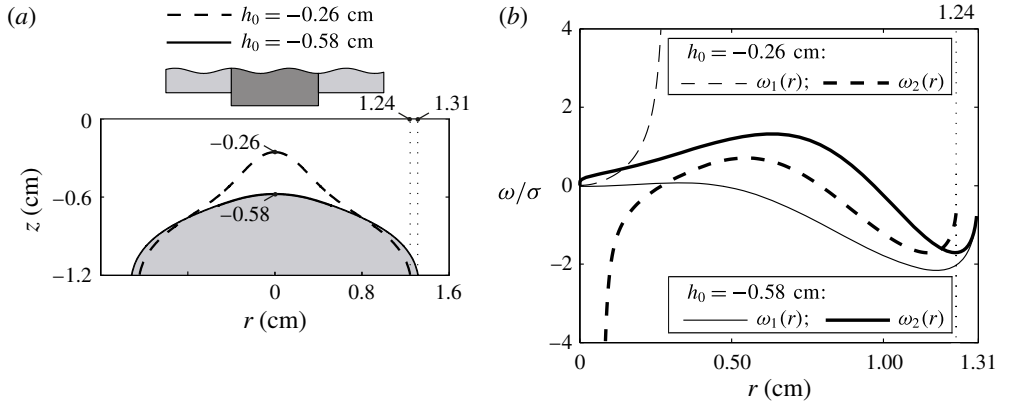

FIGURE 11. (*a*) Unstable ($h_0 = -0.26$ cm, $r_1 = 1.24$ cm) and stable ($h_0 = -0.58$ cm, $r_1 = 1.31$ cm) solutions for the drops on the lower plate at $i = 1$ A for $V_0 = 2$ cm^3, $d = 1.2$ cm and $\theta_0 = 80°$; (*b*) characteristic ω functions corresponding to these drops.

Solution branches. Here, we consider only simply connected equilibrium shapes of an MF drop on the lower plate, an MF drop on the upper plate or an MFB. For these three shape types, the dependencies of the characteristic coordinates h_0 and r_0 on i are obtained numerically for an MF volume $V_0 = 2$ cm^3 and a distance between the plates $d = 1.2$ cm, see figure 10. It can be seen that for a certain range of currents, the surface shape of the MF cannot be determined unambiguously.

For example, there are two different branches of solutions for the drop on the lower plate: more lifted and flattened, see figure 11(*a*) at $i = 1$ A. For the obtained solutions, equation (3.14) with the boundary conditions (3.15) is solved numerically. It shows that for all drops, which correspond to the branch of the more lifted solutions, the necessary and sufficient conditions of the minimum energy are not satisfied, since

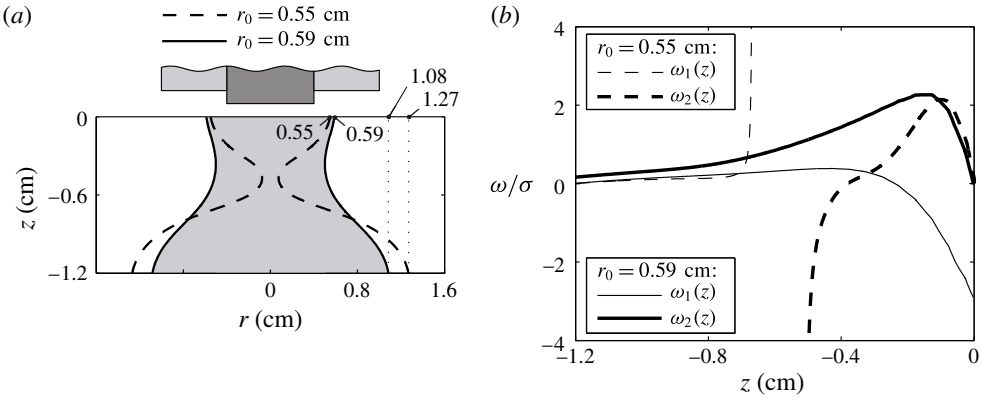

FIGURE 12. (*a*) Unstable ($r_0 = 0.55$ cm, $r_1 = 1.27$ cm) and stable ($r_0 = 0.59$ cm, $r_1 = 1.08$ cm) solutions for the MFB at $i = 0.8$ A for $V_0 = 2$ cm^3, $d = 1.2$ cm and $\theta_0 = 80°$; (*b*) characteristic ω functions corresponding to these shapes.

$\omega_2(r) - \omega_1(r) < 0$ on the intersection of the domains of these functions. An example is shown in figure 11(*b*) for $h_0 = -0.26$ cm at $i = 1$ A. According to § 3.4, it can be concluded that the local minimum of the energy functional for the obtained solutions is not reached and they are unstable. For more flattened solutions of the drop on the lower plate, the local energy minimum is reached for currents from $i = 0$ A to $i = 1.02$ A, as $\omega_2(r) - \omega_1(r) > 0$ on the whole segment $[0, r_1]$, see figure 11(*b*) for $h_0 = -0.58$ cm at $i = 1$ A. Hence, they are surface shapes stable relative to small axisymmetric surface perturbations. At currents from $i = 1.02$ A to the value $i = 1.07$ A, at which two solution branches of the drop on the lower plate intersect, the necessary and sufficient conditions of the minimum energy for the flattened drops are not satisfied, i.e. these surface shapes are unstable.

The numerical calculation of the surface shape of the MF drop retained on the upper plate beneath the coil shows that one solution branch with $V_0 = 2$ cm^3 exists on the range of currents $i \geqslant 1.8$ A, see figure 10. By checking the necessary and sufficient conditions of the energy minimum, it can be shown that from $i = 1.8$ A to $i = 1.87$ A they are not satisfied on the shapes of the upper drop. The solutions obtained for $i \geqslant 1.87$ A meet all necessary and sufficient minimum conditions, so they are stable relative to small axisymmetric surface perturbations.

For the MFB of $V_0 = 2$ cm^3, three solution branches exist, two of which do not satisfy the necessary and sufficient minimum conditions, see figure 10. The main branch is obtained for currents from $i = 0.64$ A to $i = 2.55$ A. The calculations show that MFB equilibrium surface shapes corresponding to the main branch realise the local energy minimum within the range from $i_{cr} = 0.72$ A to $i_{cr} = 2.3$ A. These marginal values are the critical currents of the MFB for $d = 1.2$ cm, at which it breaks up. Moreover, the volumes of the resulting drops on the lower and upper plates can be estimated approximately. Figure 12(*a*) illustrates two solutions of the MFB existing at $i = 0.8$ A. The one assigned with points $r_0 = 0.59$ cm and $r_1 = 1.08$ cm is stable relative to small axisymmetric surface perturbations since on it the necessary and sufficient conditions of the minimum energy are satisfied: $\omega_2(z) - \omega_1(z) > 0$ on the whole segment $[-d, 0]$, see figure 12(*b*). Recall that these characteristic functions of the MFB are determined by equations given in appendix B. On the contrary, for the other solution with $r_0 = 0.55$ cm and $r_1 = 1.27$ cm, the local energy minimum

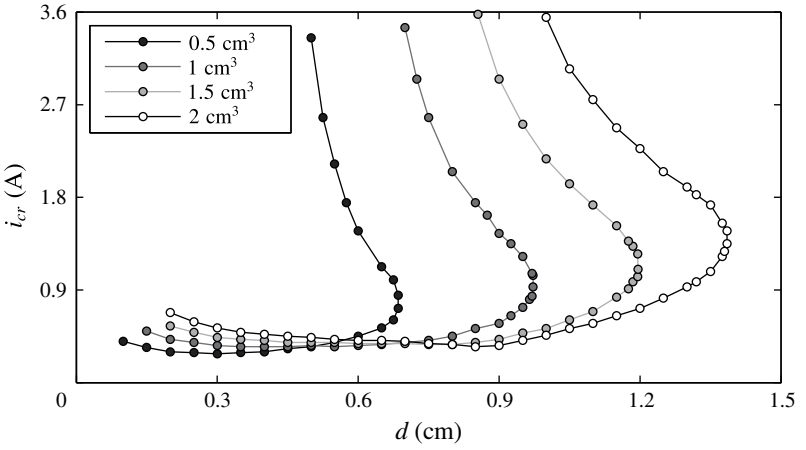

FIGURE 13. Numerically obtained stability curves $i_{cr} = i_{cr}(d)$ of the MFB of $V_0 = 0.5$ cm^3, 1 cm^3, 1.5 cm^3 and 2 cm^3 for the case of a constant contact angle $\theta_0 = 80°$.

is not reached because no common domain of $\omega_1(z)$ and $\omega_2(z)$ exists on $[-d, 0]$, see figure 12(*b*). So this MFB having a narrow neck in the middle is unstable and it would break up into two drops where the volume of each drop can be estimated from the height of the neck.

Stability curves. The theoretical method of finding stable/unstable MF surface shapes can be applied to obtain stability curves of the MFB numerically. This is accomplished as follows: for the fixed parameters d and V_0, MFB equilibrium shapes are calculated depending on the current i, that is, similar dependencies $r_0(i)$ as shown in figure 10 are computed. By checking the necessary and sufficient conditions of the energy minimum, the surface shapes stable relative to small axisymmetric surface perturbations are marked out by black on the main solution branch. Taking the marginal stable points, the critical current values $i_{cr}(d)$ of the MFB with volume V_0 are determined. The resulting stability curves $i_{cr} = i_{cr}(d)$ are presented in figure 13 for four different MF volumes. It can be seen that, although these lines are carried out for a constant contact angle of $\theta_0 = 80°$, they are qualitatively similar to the experimental dependencies in figure 8. This can be seen as a good proof of the model validity.

Thus, based on the numerical calculation of MF equilibrium shapes for $\theta_0 = \text{const.}$, it is possible to determine stability regions of the simply connected solutions and to predict qualitatively how the transformation of a given MF volume can proceed. As seen in figure 10, for a large volume of $V_0 = 2$ cm^3, the MF drop initially placed on the lower plate will become unstable at increasing $\uparrow i = 1.02$ A and most likely will abruptly form an MFB since the stability regions of these solutions have a wide intersection there. The same transformation process was observed in the experiment. However, it occurred at the other critical value $\uparrow i = 0.69$ A due to the presence of the wetting hysteresis phenomenon, see figure 6. For a lower value of V_0, if no MFB exists (figure 13), the initial drop on the lower plate will divide into two parts for increasing i. The obtained results reveal that the bistability of simply connected solutions in certain current ranges leads to the hysteresis of the MF surface.

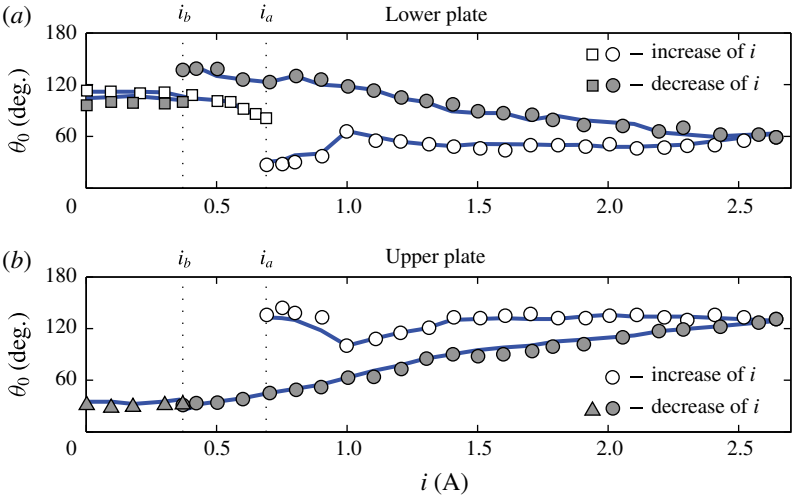

FIGURE 14. (Colour online) Contact angles $\theta_0(i)$ on the lower (a) and upper (b) plates for the MF equilibrium surface shapes of $V_0 = 2$ cm^3 shown in figure 6. Measured data: □ – drop on the lower plate; △ – drop on the upper plate; ○ – MFB. Current values at which abrupt changes occur: $\uparrow i_a = 0.69$ A and $\downarrow i_b = 0.37$ A. The solid line shows the corresponding values $\theta_0(i)$ used in numerical calculations.

4.3. *Calculation of MF equilibrium surface shapes under consideration of the wetting hysteresis phenomenon*

In order to compare stable equilibrium surface shapes of the MF obtained experimentally and theoretically, the wetting hysteresis phenomenon is taken into account. This means that the experimental dependencies of the contact angle $\theta_0(i)$ on current are used as constraints in the simulations.

Since, in terms of technical applications the stable MFB between the plates existing in wide current ranges is of particular interest, the comparison of the experimental and numerical results is made for an MF volume of $V_0 = 2$ cm^3. As was mentioned, the MF volume can have different surface forms due to the contact angle hysteresis. For example, figure 6(*d*,*f*) shows two different MFBs for the increasing and decreasing $i = 1$ A. Obviously, this is caused by the varying wetting/non-wetting contact angles, where an MF–NML interface meets the solid plate. These angles are measured by image analysis of experimental photos and plotted depending on the current in figure 14. When calculating an MF surface shape, these dependencies are applied as follows. For each current value i, the form of numerical solution to be sought is defined according to the experiment, see figure 7. Starting with the simply connected drop on the lower plate for the increasing i and then the MFB, the corresponding contact angles used in calculations are assigned values equal (or close) to the experimentally measured values $\theta_0(i)$, so that the obtained solution has a volume of $V_0 = 2$ cm^3. At the decreasing current $\downarrow i_b = 0.37$ A, when the MFB disintegrates, the volumes of the resulting upper and lower drops are estimated on the basis of the photo to be 0.13 cm^3 and 1.87 cm^3, respectively. Then, the form of these drops is calculated separately from each other taking experimental values $\theta_0(i)$.

Thus, figure 15 shows equilibrium surface shapes of this MF volume calculated considering the contact angle hysteresis for the increasing and decreasing current cases. It may be seen that the obtained surface shapes coincide with the experimental forms

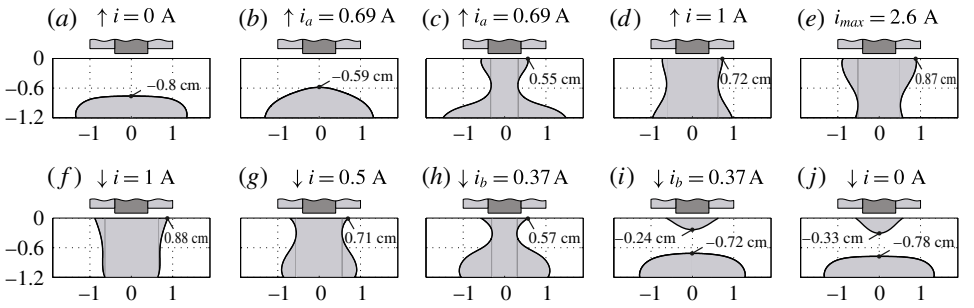

FIGURE 15. Equilibrium surface shapes of an MF volume $V_0 = 2$ cm^3 obtained numerically by taking into account the wetting hysteresis phenomenon for the increasing (*a–e*) and decreasing (*e–j*) current i.

presented in figure 6. The theoretical dependencies of the characteristic coordinates h_0 and r_0 of the drops on the upper or lower plates and of the MFB are plotted against the current i in figure 7 (bold line). It has been shown that, according to the theoretical analysis, the MF surface shapes observed in the experiment realise a local minimum of the MF energy for practically all values of the current.

5. Conclusions

The problem of the static surface shape of an MF volume between two horizontal plates in the magnetic field of an electromagnet is investigated theoretically and experimentally. The abrupt changes and hysteresis of the MF surface shape are observed in the experiments, when the current in the coil increases and decreases quasi-statically. The current values at which these abrupt changes take place are determined. The variational problem of minimum energy of a simply connected MF volume is considered theoretically. The necessary and sufficient conditions for a local minimum of the energy functional are derived, from which the method to find stable/unstable MF surface shapes is developed. In the case of a constant contact angle, MF equilibrium surface shapes are calculated numerically with the unstable solutions picked out. The stability curves of the MFB are determined theoretically for a constant contact angle. It is shown that these dependencies are qualitatively similar to the experimental stability curves. The MF equilibrium surface shapes are obtained numerically taking into account the wetting hysteresis phenomenon, which is observed in the experiment for the increasing and decreasing current. It is found that the experimental surface shapes coincide with the shapes obtained numerically, and practically all of them satisfy the derived necessary and sufficient conditions of the minimum energy. The obtained results can be used to design applications based on MF, such as valves, interrupters and cooling systems.

Acknowledgements

This work is supported financially by the Russian Foundation for Basic Research (RFBR) within the project 16-51-12024, as well as by the research association between the Deutsche Forschungsgemeinschaft (DFG) and the RFBR within PAK907 under the project PO2013/1-1. The authors are grateful to Dr V. Böhm (TU Ilmenau) for his help with finite element method simulations.

Appendix A

For the MF drop on the upper plate with the axisymmetric surface shape $z = h(r)$, the auxiliary functional $\Psi[h]$ is described according to (3.1) and (3.5) as

$$\Psi[h] = 2\pi \int_0^{r_1} f(r, h, h')\,\mathrm{d}r, \quad \text{where } f(r, h, h') = \sigma r\sqrt{1 + h'^2(r)} - \sigma r\cos\theta_0 - \frac{1}{2}grh(r)(\rho_1 - \rho_2)(h(r) + 2d) + nkT\int_0^{h(r)} r\ln\frac{\sinh(mH(r, z)/(kT))}{mH(r, z)/(kT)}\,\mathrm{d}z + p_0 rh(r). \tag{A 1}$$

Here, $(r_1, 0)$ is the point of intersection of the surface $z = h(r)$ with the upper plate.

Appendix B

For the MFB between the plates with the surface shape function $r = \zeta(z)$, the auxiliary functional $\Psi[\zeta]$ has the following form:

$$\Psi[\zeta] = F[\zeta] - p_0 V_0[\zeta] = 2\pi\int_{-d}^{0} f(z, \zeta, \zeta')\,\mathrm{d}z - \pi\sigma\cos\theta_0(\zeta^2(0) + \zeta^2(-d)), \tag{B 1}$$

where

$$f(z, \zeta, \zeta') = \sigma\zeta(z)\sqrt{1 + \zeta'^2(z)} + \frac{1}{2}g\zeta^2(z)(\rho_1 - \rho_2)(z + d) - nkT\int_0^{\zeta(z)} r\ln\frac{\sinh(mH(r, z)/(kT))}{mH(r, z)/(kT)}\,\mathrm{d}r - \frac{1}{2}p_0\zeta^2(z). \tag{B 2}$$

In this case, the equation for the determination of the characteristic functions $\omega_1(z)$ and $\omega_2(z)$ is

$$f''_{\zeta'\zeta'}\left(f''_{\zeta\zeta} - \frac{\mathrm{d}}{\mathrm{d}z}f''_{\zeta\zeta'} + \omega'(z)\right) = \omega^2(z). \tag{B 3}$$

Taking into account the explicit form of $f(z, \zeta, \zeta')$, it can be seen that the boundary conditions for these functions are identically zero:

$$\omega_1(-d) = f''_{\zeta\zeta'}|_{z=-d} + \sigma\cos\theta_0 = 0 \quad \text{and} \quad \omega_2(0) = f''_{\zeta\zeta'}|_{z=0} - \sigma\cos\theta_0 = 0. \tag{B 4a,b}$$

REFERENCES

Abou, B., Wesfreid, J.-E. & Roux, S. 2000 The normal field instability in ferrofluids: hexagonsquare transition mechanism and wavenumber selection. *J. Fluid Mech.* **416**, 217–237.

Afkhami, S., Tyler, A. J., Renardy, Y., Renardy, M., Pierre, T. G. St., Woodward, R. C. & Riffle, J. S. 2010 Deformation of a hydrophobic ferrofluid droplet suspended in a viscous medium under uniform magnetic fields. *J. Fluid Mech.* **663**, 358–384.

Arkhipenko, V. I., Barkov, Yu. D. & Bashtovoi, V. G. 1980 Behavior of a drop of a magnetizable liquid in magnetic fields. *Magnetohydrodynamics* **16**, 221–227.

Bacri, J.-C., Frenois, C., Perzynski, R. & Salin, D. 1988 Magnetic drop-sheath wetting transition of a ferrofluid on a wire. *Rev. Phys. Appl.* **23**, 1017–1022.

Bacri, J.-C. & Salin, D. 1982 Instability of ferrofluid magnetic drops under magnetic field. *J. Phys. Lett.* **43**, 649–654.

BARKOV, YU. D. & BERKOVSKII, B. M. 1980 Breakup of a drop of magnetic fluid. *Magnetohydrodynamics* **16**, 228–230.

COWLEY, M. D. & ROSENSWEIG, R. E. 1967 The interfacial stability of a ferromagnetic fluid. *J. Fluid Mech.* **30**, 671–688.

GAILITIS, A. 1977 Formation of the hexagonal pattern on the surface of a ferromagnetic fluid in an applied magnetic field. *J. Fluid Mech.* **82**, 401–413.

GELFAND, I. M. & FOMIN, S. V. 2000 *Calculus of Variations*. Dover Publications.

DE GENNES, P. G. 1985 Wetting: statics and dynamics. *Rev. Mod. Phys.* **57**, 827–863.

JOHN, T., RANNACHER, D. & ENGEL, A. 2007 Influence of surface tension on the conical meniscus of a magnetic fluid in the field of a current-carrying wire. *J. Magn. Magn. Mater.* **309**, 31–35.

KIRYUSHIN, V. V. & BIN, C. Z. 1980 Figures of equilibrium of a magnetizable fluid in a magnetic field. *Fluid Dyn.* **15**, 573–578.

LANDAU, L. D. & LIFSHITZ, E. M. 1980 *Electrodynamics of Continuous Media*. Pergamon.

NALETOVA, V. A., KIRYUSHIN, V. V., REKS, A. G. & SUVCHUK, E. 2008 Hysteresis of a shape of a magnetic fluid volume near a line conductor. *Magnetohydrodynamics* **44**, 167–174.

NALETOVA, V. A., TURKOV, V. A., PELEVINA, D. A., ROZIN, V. A., ZIMMERMANN, K., POPP, J. & ZEIDIS, I. 2012 Behavior of a free surface of a magnetic fluid containing a magnetizable cylinder. *J. Magn. Magn. Mater.* **324**, 1253–1257.

PLATEAU, J. 1863 Experimental and theoretical researches on the figures of equilibrium of a liquid mass withdrawn from the action of gravity. In *Annual Report of the Board of Regents of the Smithsonian Institution*, pp. 207–285. Government Printing Office.

POLEVIKOV, V. & TOBISKA, L. 2005 Instability of magnetic fluid in a narrow gap between plates. *J. Magn. Magn. Mater.* **289**, 379–381.

RICHTER, R. & LANGE, A. 2009 Surface instabilities of ferrofluids. In *Colloidal Magnetic Fluids: Basics, Development and Application of Ferrofluids* (ed. S. Odenbach), Lect. Notes Phys., vol. 763, pp. 157–247. Springer.

ROSENSWEIG, R. E. 1985 *Ferrohydrodynamics*. Cambridge University Press.

ROSENSWEIG, R. E., ELBORAI, S., LEE, S.-H. & ZAHN, M. 2005 Ferrofluid meniscus in a horizontal or vertical magnetic field. *J. Magn. Magn. Mater.* **289**, 192–195.

ROTHERT, A. & RICHTER, R. 1999 Experiments on the breakup of a liquid bridge of magnetic fluid. *J. Magn. Magn. Mater.* **201**, 324–327.

VINOGRADOVA, A. S., NALETOVA, V. A., TURKOV, V. A. & REKS, A. G. 2013 Influence of apex angles of limiting conic surfaces on the hysteresis of the shape of a magnetic fluid drop on a line conductor. *Magnetohydrodynamics* **49**, 350–354.

VOLKOVA, T. I. & NALETOVA, V. A. 2014 Instability of the magnetic fluid shape in the field of a line conductor with current. *Fluid Dyn.* **49**, 3–10.

VOLKOVA, T. I., NALETOVA, V. A. & TURKOV, V. A. 2013 Magnetic fluid volume between horizontal plates in the field of an electromagnetic coil. *Magnetohydrodynamics* **49**, 386–390.

YILDIRIM, O. E. & BASARAN, O. A. 2001 Deformation and breakup of stretching bridges of newtonian and shear-thinning liquids: comparison of one- and two-dimensional models. *Chem. Engng Sci.* **56**, 211–233.

ZAHN, M. 2001 Magnetic fluid and nanoparticle applications to nanotechnology. *J. Nanopart. Res.* **3**, 73–78.